NUCLEAR THEORY, Vol. 35 (2016)
eds. M. Gaidarov, N. Minkov, Heron Press, Sofia

Phases and Phase Transitions in the Algebraic Microscopic Pairing-plus-Quadrupole Model: Role of the Single-Particle Term in the Hamiltonian

K.P. Drumev[1], **A.I. Georgieva**[2], **J. Cseh**[3]

[1]Institute for Nuclear Research and Nuclear Energy,
Bulgarian Academy of Sciences, 1784 Sofia, Bulgaria

[2]Institute of Solid State Physics, Bulgarian Academy of Sciences,
1784 Sofia, Bulgaria

[3]Institute for Nuclear Research of the Hungarian Academy of Sciences,
P.O. Box 51, H-4001 Debrecen, Hungary

Abstract. The possibility of describing phases and phase transition phenomena in nuclear systems is discussed in the context of a symmetry-adapted shell-model study. We perform calculations within the Extended Microscopic Algebraic Pairing-plus-Quadrupole Shell Model and present the outcome for two sd-shell isotopes: ^{20}Ne and ^{20}O. Results for the best-fit description of the excitation spectrum demonstrate the effects on the systems coming from the addition of the single-particle spin-orbit interaction to the pairing-plus-quadrupole Hamiltonian.

1 Introduction

Symmetry-adapted shell models are considered as an appropriate tool to study the quantum phases and the phase transitions in finite quantum systems [1]. Usually, this kind of models have limiting cases (dynamical symmetries) which give analytical solution. When one deals with a Hamiltonian which has nonzero contributions from two (or more) interactions of different dynamical symmetries, a numerical solution is required. The relative weight of the dynamically symmetric interactions serves as a control parameter and it defines the phase diagram of the system.

The quadrupole-quadrupole interaction has been a standard ingredient in nuclear structure models that aim at reproducing rotational spectra and nuclear deformations. It emerges as a leading contribution in the multipole expansion of any nuclear long-range potential. It is essential for modeling collective properties of nuclei such as reduced quadrupole transition rates and quadrupole moments. One model which makes use of the dominance of the quadrupole-quadrupole interaction in deformed nuclei is the Elliott's $SU(3)$ shell model [2].

Similarly, the pairing interaction has long been known to play an important role in the physics of many-body systems. For its description, the single j-shell seniority coupling scheme [3] and its multiple j-shell generalization [4] are employed to obtain an exact solution. In this case, the seniority quantum number (generalized seniority for the multiple $j-$shell case) v, which counts the number of unpaired nucleons, governs the complexity of the problem. Unfortunately, pair breaking in nuclei, as generated for example by the spin-orbit interaction, is known to be very important. Since the complexity of the scheme grows combinatorially with v, this approach is problematic for all but near closed shell systems.

Although in some nuclei the pairing and the quadrupole interactions could reproduce relatively well the observed behavior of the nuclear system, in most of the cases the study of the relationship between them is of great importance. This is the main motivation for the development of the Pairing-plus-Quadrupole Model (PQM) [5] for the description of the nuclear excitation spectra.

Along the last five years, an algebraic approach was developed [6–10] by considering the basic interactions of the PQM as invariants of the respective algebras, which reduce the general symmetry of the shell model in a dynamical way. At the same time, the so defined dynamical symmetry chains are complementary to the Wigner's spin-isospin $SU_{ST}(4)$ [11] symmetry, which establishes direct connections between the limiting cases These dynamical symmetries could be considered as different phases of the nuclear structure. In the lower shells up to mass numbers $A \sim 100$, the two modes – the pairing and the quadrupole interactions – compete, and in this way different types of collective spectra, ranging between vibrational and rotational, can be investigated in terms of phase transitions [12]. In this way, we establish the mixing of the $SU(3)$ basis states into the pairing bases.

As a symmetry-adapted model, the above approach is a reasonable candidate for a model, suitable to describe the phases and the phase transition phenomena. In this particular work, we study and illustrate the role that the introduction of the one-body spin-orbit term in the Hamiltonian plays in the reproduction of the spectra in realistic nuclear systems. Spin-orbit correlations were first introduced independently by Mayer [13] and by Haxel, Jensen, and Suess [14] in order to explain shell closures and magic numbers. In any given harmonic oscillator shell, the spin-orbit force mainly affects the largest-j orbital by lowering it energetically. In heavy nuclei, where the effect is so strong that magic numbers deviate from the major shell closures of the harmonic oscillator, the pseudo-spin concept can be applied [15].

We investigate the effect of the l.s coupling on the spectra of two sd-shell systems – the nuclei ^{20}Ne and ^{20}O. Finally, we translate our results in terms of appropriately introduced control parameters and try to relate them with the concept of phases and the description of phase transition phenomena.

2 The Model

In our earlier works [8–10], the algebraic structure of the shell-model algebra $U(4\Omega)$ is investigated to obtain its reductions through the microscopic pairing algebra $SO(\Omega) \sim SO(8)$, containing all the limits of the $SO(8)-$ pairing model and the Elliott's $SU(3)$ algebra. The generators of the latter are the quadrupole $Q_\mu = \sum_l \sqrt{8(2l+1)}(a^\dagger{}_{l\frac{1}{2}\frac{1}{2}} \times \tilde{a}_{l\frac{1}{2}\frac{1}{2}})^{(200)}_{(\mu 00)}$ and the angular momentum $L_\mu = \sum_l \sqrt{4l(2l+1)(l+1)/3}(a^\dagger{}_{l\frac{1}{2}\frac{1}{2}} \times \tilde{a}_{l\frac{1}{2}\frac{1}{2}})^{(100)}_{(\mu 00)}$ operators, expressed in terms of individual nucleon coordinate and momentum variables. Also, they are related to the collective models since the β, γ shape parameters can be easily expressed using the labels λ and μ which describe the $SU(3)$ representations [16]. Hence, the $SU(3)$ classification of the many-body states has the advantage of allowing for a geometrical analysis of the eigenstates of a nuclear system. In $U(4\Omega)$, we obtain four reduction schemes, in which as distinct dynamical symmetries of the shell model algebra appear the $SU(3)$ algebra [16] and one of the branches of the $SO(8)$ is locally isomorphic to $SO(\Omega)$ pairing algebra [17]. This allows the classification of the basis states of the system along each of them. A relation between these chains is established on the basis of the complementarity to the Wigner's spin-isospin $U_{ST}(4) \supset U_S(2) \otimes U_T(2)$ reduction. This elucidates the algebraic structure of an extended Pairing-plus-Quadrupole Model, realized in the framework of the Elliott's SU(3) scheme [16]. Consequently, all chains determine full-basis sets and could be expressed through each other [8]. The basis states labeled by the quantum numbers of the representations of the algebras in the SU(3) chain $|\Psi_R\rangle \equiv |\{f\}\alpha(\lambda,\mu)KL,S;JM\rangle$ are eigenstates of the rotational limit of the model with quadrupole-quadrupole interaction. Correspondingly, the basis states in which the pairing interaction is diagonal [17] are labeled as $|\Psi_P\rangle \equiv |\{f\}v[p_1,p_2,p_3]\xi L,S;JM\rangle$. In the above states, $v[p_1,p_2,p_3]$ are the representations of the $SO(8)$ algebra, α, ξ and K give the multiplicity labels of the corresponding reductions. Using the expansion of the pairing states in the $SU(3)$ basis states and the diagonalization procedure for its matrix in the $SU(3)$ basis, we obtain numerically the probability with which the states of the $SU(3)$ basis enter into the expansion of the pairing bases.

The specificity of the current approach is to use a Hamiltonian that combines the quadrupole-quadrupole interaction with both the isoscalar and the isovector pairing terms, something not done in any previous applications. In an earlier work [8], the important result that the spatial subalgebra $U(\Omega)$ of the shell-model algebra $U(4\Omega)$ contains two distinct dynamical symmetries, defined by the reduction chains: a branch through $SO(\Omega)$ and another branch through $SU(3)$, was obtained. Consequently, both chains determine full-basis sets and could be expressed through each other. Further interactions may be added depending on the phenomena we need to describe.

2.1 The Hamiltonian

By comparison with some earlier works [8, 9], here we use a Hamiltonian with four ingredients of the form

$$H = \mathbf{G_0 S}^{\dagger}.\mathbf{S} + \mathbf{G_1 P}^{\dagger}.\mathbf{P} - \frac{\chi}{\mathbf{2}}\mathbf{Q}.\mathbf{Q} - \mathbf{C}\sum_{\mathbf{i}} \mathbf{l_i}.\mathbf{s_i}, \tag{1}$$

where the four parameters χ, $\mathbf{G_0}$, $\mathbf{G_1}$ and C are the strengths of the quadrupole-quadrupole, the isoscalar pairing, the isovector pairing and the single-particle spin-orbit term, respectively. The fourth term is added here and for the first time we want to explore its role in the overall description of the system. The pair creation operators that appear in this Hamiltonian are of the form

$$S^{\dagger}_{\mu} = \sum_{l} \beta_l \sqrt{\frac{2l+1}{2}} [a^{\dagger}_{l\frac{1}{2}\frac{1}{2}} \times a^{\dagger}_{l\frac{1}{2}\frac{1}{2}}]^{010}_{0\mu 0} \tag{2}$$

and

$$P^{\dagger}_{\mu} = \sum_{l} \beta_l \sqrt{\frac{2l+1}{2}} [a^{\dagger}_{l\frac{1}{2}\frac{1}{2}} \times a^{\dagger}_{l\frac{1}{2}\frac{1}{2}}]^{001}_{00\mu}, \tag{3}$$

where the phase factors $\beta_l = +1$ or -1, and the bracket denotes coupling in the angular momentum, spin and isospin [17].

2.2 The symmetry triangle and the symmetry tetrahedron

The relative weights of the interactions entering the eq. (1) serve as control parameters and define the phase diagram of the system. In the case, when there are more than two dynamical symmetries, more than one control parameters should be introduced.

The quadrupole interaction has $SU(3)$ dynamical symmetry. A simple model of the isovector and isoscalar pairing can be obtained in an L, S, T scheme which has $SO(8)$ dynamical symmetry. Next, the pairing-plus-quadrupole interactions define a submodel with a phase-space of two dimensions (two control parameters), which can be illustrated by a triangle. Each corner corresponds to a dynamical symmetry in the L, S, T scheme in the Wigner's supermultiplets: one of them is the $SU(3)$, and the others are the isoscalar and the isovector pairing interactions. Hence, analytical solutions are available for the total pairing, with isoscalar and isovector interactions with equal strenghts, the pure isoscalar $SO_S(5)$ and for the pure isovector $SO_T(5)$ interactions [4]. (Note that the $SO(5)$ algebra is isomorphic with the $Sp(4)$ (compact symplectic) algebra [20], and $SU(4)$ is isomorphic with $SO(6)$.) A possible convenient choice for the two control parameters are: x, where the relative strength of the two kinds of pairing are $G_0 = xG, G_1 = (1-x)G, 0 \leq x \leq 1$, and y for the relative weight of the quadrupole and the pairing strength G are $\chi = y\chi_p, G = (1-y)\chi_p, 0 \leq y \leq 1$),

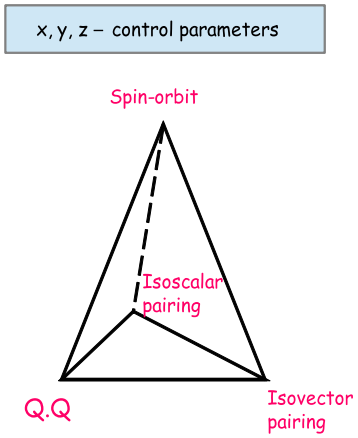

Figure 1. The symmetry tetrahedron.

where $\chi_p = \chi + G_0 + G_1$. As a result the phase diagram is a triangle, where the three limiting cases at its vertices are defined by the conditions: $y = 1, x-$ arbitrary for the $SU(3)$ limit, $x = 1, y = 0$ for the isoscalar case and $x = 0, y = 0$ for the isovector one. By means of their values we can evaluate the role of each of the three interactions in the description of the realistic nuclear spectra in each nucleus.

The increasing strength of the spin-orbit force destroys the $L - S$ coupling and the system prefers the $j-j$ coupling. This adds a new dimension in the phase diagram (see Figure 1), which turns to a three-dimensional one, illustrated by a tetrahedron. The distance from the $L - S$ plain $(1 - z)$ can be chosen as the third control parameter. For convenience, we measure it from the $SU(3)$ corner, introducing the following control parameter: $C = (1 - z)\chi_{max}$, $\chi_p = z\chi_{max}$, where $0 \leq z \leq 1)$. This last parameter $\chi_{max} = \chi + G_0 + G_1 + C$ is called the scale parameter. Obviously, at $z = 1$ $C = 0$ and the two-parameter case (the triangle) is restored. At $z = 0$, only the $l.s$ term remains and for arbitrary $z, 0 \leq z \leq 1)$, the Hamiltonian (1) can be rewritten as

$$H = \chi_{max}\{-\tfrac{yz}{2}Q.Q + x(1-y)zS^{\dagger}.S + (1-x)(1-y)zP^{\dagger}.P - (1-z)\textstyle\sum_i l_i.s_i)\}. \quad (4)$$

The above phase diagrams allow us to investigate the influence of these residual (in respect to the nuclear mean field) interactions on the spectra in real nuclear systems.

3 Results

In this work, we deal with a real test case for the applications of the theory – the sd-shell, which is the first one, where both deformation and pairing phenomena

play an important role [21, 22]. Our proof-of-case example presents the simple but complete system of 4 particles in the sd-shell which allows us to study the PQM without any truncation of the model space.

The calculations are performed in the $SU(3)$ basis which has the form $|\Psi_R\rangle \equiv |\{f\}\alpha(\lambda,\mu)KL,S;JM\rangle$ where α and K give the multiplicity labels of the corresponding reductions. We use techniques for generating the list of the $SU(3)$ representations [23] and calculating the $SU(3) \times SU(2)$ reduced matrix elements from [24] to evaluate each part of the Hamiltonian in the basis. This is followed by a numerical diagonalization of the obtained matrix which results in finding the energy spectrum and the eigenstates of the system.

We can demonstrate the complementarity of the two competing modes (the pairing and the quadrupole one) by showing the energy spectrum calculated with the Hamiltonian (1) but this time the results might be affected by the presence of the single-particle spin-orbit term. A best-fit parameter estimate is done using the 21 lowest-lying positive-parity states in ^{20}Ne and the 12 lowest-lying positive-parity states in ^{20}O from the experiment [25]. The quality of the fit has been estimated using the root mean squared /RMS/ deviation of the model energies from the experimental ones $\sigma = \sqrt{\sum_i (E^i_{Th} - E^i_{Exp})^2/d}$ (with $d = N - p$, where N – number of experimental points, p – number of parameters in the fit).

Below, we perform two types of calculations. For both nuclei, we can do a three-parameter case, where for the ^{20}Ne nucleus the isoscalar and the isovector pairing are forced to have equal strengths, while for ^{20}O only the isovector pairing is present. In the second type of calculation, doable only for the nucleus ^{20}Ne, the pairing strengths are separated and allowed to vary independently with C appearing as a fourth fitting parameter.

3.1 Results with the spin-orbit interaction added as a third parameter

3.1.1 ^{20}Ne results

In this case, the result for the RMS trend is presented in Figure 2. The RMS minimum of $\sigma = 1.47$ MeV is achieved at the following best-fit parameter val-

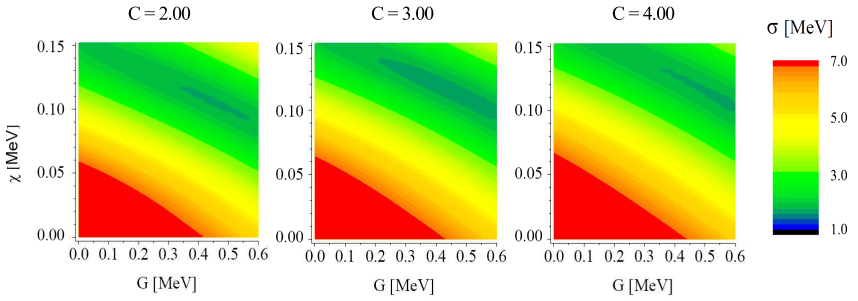

Figure 2. Results for the RMS deviation in ^{20}Ne with 3 parameters.

ues: $G = 0.44$ MeV, $\chi = 0.10$ MeV, and $C = 3.11$ MeV. Compared to the earlier two-parameter results ($G = 0.29$ MeV, $\chi = 0.11$ MeV), we have a better defined minimum, a better description of the spectrum (expressed in terms of the absolute RMS value). Also, the valley of the minima is still preserved in the presence of the spin-orbit term in the interaction Hamiltonian.

3.1.2 ^{20}O results

For this isotope, the result for the RMS trend is presented in Figure 3. The RMS minimum of $\sigma = 0.85$ MeV is achieved at the following parameter values: $G_1 = 0.20$ MeV, $\chi = 0.12$ MeV, and $C = 1.53$ MeV. Compared with the result obtained without the use of the spin-orbit interaction ($G_1 = 0.31$ MeV, $\chi = 0.15$ MeV), one again sees that the major effect is again the fact that the minimum is more clearly defined. Unlike the ^{20}Ne result above, here with the rise of C the valley of the minima moves down towards smaller values of the isovector pairing strength G_1 and the quadrupole strength χ. Also, for the points below this valley, the RMS values rarely go above 5 MeV as this happens only for very negligible values of the parameter C.

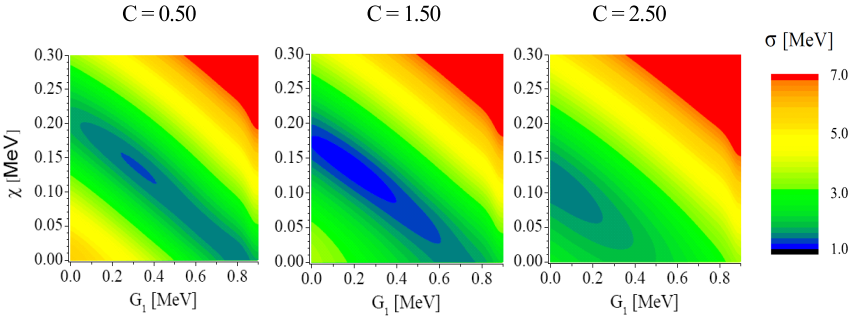

Figure 3. Results for the RMS deviation in ^{20}O with 3 parameters.

3.2 ^{20}Ne results with the spin-orbit interaction added as a fourth parameter

At last, we present the result for the ^{20}Ne isotope in the four-parameter case when the two pairing modes are allowed to participate with different strengths in the Hamiltonain. The results are presented In Figure 4, where we illustrate the trends in the description depending on the quadrupole strength χ (in up-down direction) and on the spin-orbit strength C (going left-right).

The best result is achieved at $G_0 = 0.00$ MeV, $G_1 = 0.48$ MeV, $\chi = 0.12$ MeV, and $C = 3.26$ MeV with an RMS best value of $\sigma = 1.71$ MeV (the three-parameter outcome is $G_0 = 0.29$ MeV, $G_1 = 0.29$ MeV, $\chi = 0.11$ MeV). We see that this point moves from the situation where the two pairing modes are equally present to a result where the isovector pairing should dominate in

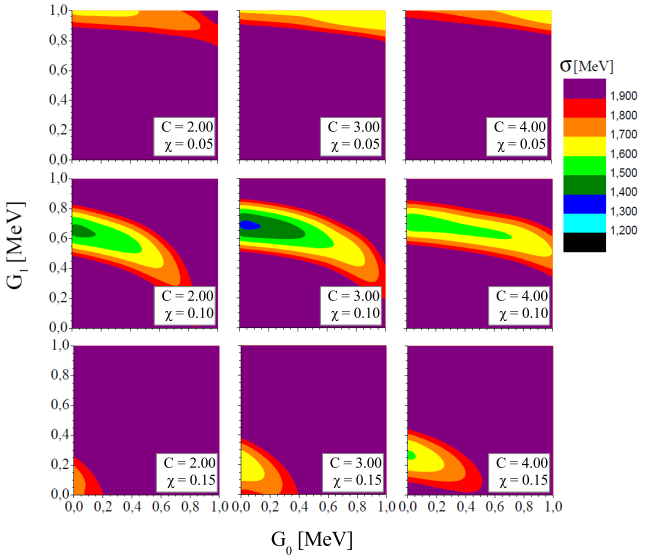

Figure 4. Results for the RMS deviation in ^{20}Ne with 4 parameters.

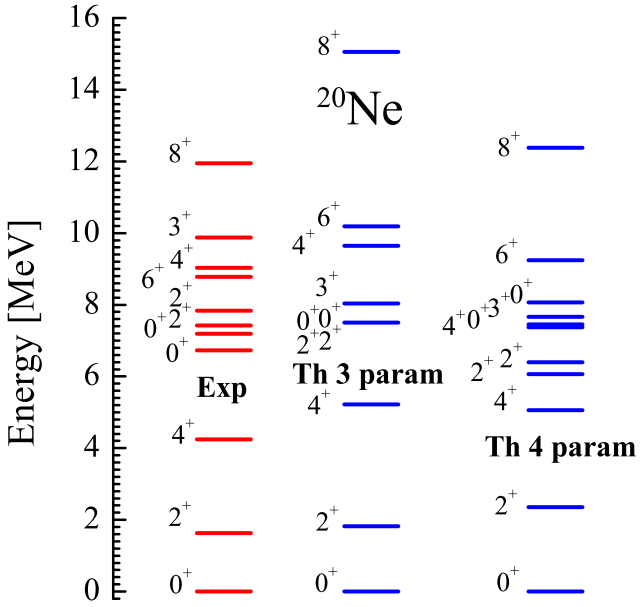

Figure 5. ^{20}Ne spectrum – the left column represents the experiment [25], followed by the 3-parameter-fit result and the one using all 4 parameters.

the four-parameter estimate. This happens at very low values of the spin-orbit strength, followed by deepening the minimum at higher C values.

The outcome we obtain is probably due to the fact that we work in the sd-shell and the $SO(\Omega)$ where the spatial degeneracy is $\Omega = 6$. So, the presence of both the isovector and the isoscalar mode appears to naturally be suppressed. In contrast, for the case for the fp shell, for example, we have dimension of $\Omega = 10$. There we expect that both pairing modes may be equally present, so it is reasonable to expect that both modes can again be allowed to be present at some comparable extent.

In Figure 5, one can compare the results for the excitation spectrum obtained using only three fitting parameters (without C) and the four-parameter result from this work. For some of the states in the spectrum, there is some clear improvement in the position of the theoretically obtained energies.

And finally, in terms of the three control parameters x, y and z, the three- and the four-parameter results are the following: $x = 0.00$, $y = 0.20$, and $z = 0.16$ versus the previous three-parameter-fit result of $x = 0.50$ and $y = 0.16$, respectively. The result is considerably different from the one obtained without the use of the spin-orbit term mainly due to the suppresion of the isoscalar phase.

4 Summary

In this work, we illustrated how the introduction of the single-particle terms in the Hamiltonian of the system affects the results obtained for the energy spectra of two sd-shell nuclei. Some of the previously observed features are preserved, others are not. The minima of the RMS deviation from the experiment with the extended Hamiltonian are better defined while the valleys of minima are reasonably well preserved in shape although they may change their position. In the four-parameter case of ^{20}Ne we show in details how the minimum drastically changes its position and express the outcome in terms of the control parameters which define the dominating symmetry(phase) of the system. Further developments of similar description of phases and transition phenomena will shortly be underway.

Acknowledgements

This work was supported by the Bulgarian National Foundation for Scientific Research under Grant Number DFNI-E02/6 (12.12.2014) and in part by the Hungarian Scientific Research Fund – OTKA (Grant No. K 112962).

References

[1] P. Cejnar, F. Iachello, *J. Phys. A* **40** (2007) 581; J. Cseh, J. Darai, H. Yepez-Martinez, P.O. Hess, *Int. J. Mod. Phys. E* **617** (2008) 2296; P. Cejnar, J. Jolie, *Progr. Part. Nucl. Phys.* **62** (2009) 210; F. Iachello, *J. Phys. Conf. Ser.* **237** (2010) 012014.

[2] J.P. Elliott, *Proc. Roy. Soc. London, Ser. A* **245** (1958) 128; **245** (1958) 562.

[3] B.H. Flowers, *Proc. Roy. Soc. London, Ser. A* **212** (1952) 248.

[4] K.T. Hecht, *Ann. Rev. Nucl. Sci.* **23** (1973) 123.

[5] S.T. Belyaev, *Mat. Fys. Medd. Dan. Vid. Selsk.* **31** No. 11 (1959); L.S. Kisslinger and R.A. Sorensen, *Rev. Mod. Phys.* **35** (1963) 853; M. Baranger and K. Kumar, *Nucl. Phys.* **62** (1965) 113.

[6] K.P. Drumev, A.I. Georgieva, NUCLEAR THEORY, Vol. **30** (2011) 189, Proceedings of the 30 International Workshop on Nuclear Theory, 26 June – 2 July 2011, eds. A. Georgieva, N. Minkov, Heron Press, Sofia.

[7] K.P. Drumev, A.I. Georgieva, NUCLEAR THEORY **31** (2012) 215, Proceedings of the 31 International Workshop on Nuclear Theory, 24 – 30 June 2012, eds. A. Georgieva, N. Minkov, Heron Press, Sofia.

[8] K.P. Drumev, A.I. Georgieva, NUCLEAR THEORY **32** (2013) 151, Proceedings of the 32 International Workshop on Nuclear Theory, 24 – 29 June 2013, eds. A. Georgieva, N. Minkov, Heron Press, Sofia.

[9] K.P. Drumev, A.I. Georgieva, NUCLEAR THEORY **33** (2014) 162, Proceedings of the 33 International Workshop on Nuclear Theory, 22 – 28 June 2014, eds. A. Georgieva, N. Minkov, Heron Press, Sofia.

[10] K.P. Drumev, A.I. Georgieva, NUCLEAR THEORY **34** (2015) 115, Proceedings of the 34 International Workshop on Nuclear Theory, 21 – 27 June 2015, eds. M. Gaidarov, N. Minkov, Heron Press, Sofia; `http://ntl.inrne.bas.bg/workshop/2015/contributions/`

[11] E.P. Wigner, *Phys. Rev.* **51** (1937) 106.

[12] J. Cseh, *J. Phys. Conf. Ser.* **205** (2010) 012021.

[13] M.G. Mayer, Phys. Rev. 75 (1949) 1969.

[14] O. Haxel, J.H.D. Jensen, H.E. Suess, Phys. Rev. 75 (1949) 1766.

[15] R.D. Ratna Raju, J.P. Draayer and K.T. Hecht, Nucl. Phys. **A202** (1973) 433.

[16] J.P. Draayer, in *Algebraic Approaches to Nuclear Structure: Interacting Boson and Fermion Models*, Contemporary Concepts in Physics VI, edited by R.F. Casten (Harwood Academic, Chur, Switzerland) (1993) 423.

[17] V.K.B. Kota, J.A. Castilho Alcaras, *Nucl. Phys.* **A764** (2006) 181.

[18] A. Bohr, B.R. Mottelson, and D. Pines, *Phys. Rev.* **110** (1958) 936.

[19] R.D. Ratna Raju, J.P. Draayer, K. T. Hecht, *Nucl. Phys.* **A202** (1973) 433.

[20] H.J. Lipkin, Lie groups for pedestrians, North-Holland, Amsterdam (1966) 69.

[21] J.P. Elliott and M. Harvey, *Proc. Roy. Soc. London, Ser. A* **272** (1963) 557; J.P. Elliott and C.E. Wisdon, *Proc. Roy. Soc. London, Ser. A* **302** (1968) 509.

[22] C.E. Vargas, J.G. Hirsch, J.P. Draayer, *Nucl. Phys.* **A690** (2001) 409.

[23] J.P. Draayer, Y. Leschber, S.C. Park, and R. Lopez, *Comput. Phys. Commun.* **56** (1989) 279.

[24] C. Bahri, J.P. Draayer, *Comput. Phys. Commun.* **83** (1994) 59; Y. Akiyama and J.P. Draayer, *Comput. Phys. Commun.* **5** (1973) 405.

[25] `http://www.nndc.bnl.gov/`